Wear Maps of Si_3N_4 Ceramic Cutting Tool

Y.-R. Liu, J.-J. Liu, B.-L. Zhu, Z.-R. Zhou, L. Vincent, and P. Kapsa

Wear maps of a Si_3N_4 ceramic cutting tool for cutting 1045 plain carbon and 302 stainless steels are produced in this paper. Through the systematic turning tests, the optimum cutting regions were determined on the wear maps of a two-dimensional diagram of cutting speed and feed rate. They are important for selecting the appropriate cutting parameters for a ceramic tool when cutting different workpieces. The wear morphologies and wear mechanisms for the different regions were investigated by scanning electron microscopy (SEM) with energy dispersive analysis of x-ray (EDX), and the corresponding cutting temperature distributions were measured by a thermal video system. Based on the experiment results, the relationships between cutting conditions, cutting temperatures, and wear mechanisms were discussed in detail.

Keywords ceramic cutting tools, wear map, wear mechanisms

1. Introduction

Ceramic cutting tools have been widely used for high speed finishing and high removal rate because of their unique mechanical properties, especially at elevated temperatures (Ref 1-5). Their wear life is much longer than conventional cemented carbide and high speed steel tools (Ref 6-9). However, this does not mean that ceramic tools can effectively machine any kind of workpiece at any cutting condition (Ref 10, 11). Tool wear and fracture usually occur when applying the ceramic tool in an incorrect way. To diminish tool wear and fracture that decreases machining accuracy, shortens tool life, and lowers productivity, it is important to employ tools in appropriate conditions, which can be determined through fundamental research on the relationship between cutting conditions, cutting temperatures, and wear mechanisms. In this paper, the wear maps of Si_3N_4 ceramic cutting tools for cutting 1045 plain carbon and 302 stainless steels were investigated to provide the basis for reasonable utilization and to reveal the wear mechanisms at different cutting conditions.

Y.-R. Liu, J.-J. Liu, and **B.-L. Zhu,** Tribology Research Institute, Tsinghua University, Beijing 100084, People's Republic of China; **Z.-R. Zhou,** Southwest Jiaotong University, Chengdu 610031, People's Republic of China; and **L. Vincent** and **P. Kapsa,** Ecole Centrale De Lyon, 69131 Ecully, Cedex, France.

Table 1 Chemical composition and mechanical properties of Si_3N_4 cutting tool

Chemical composition	Hardness, HRA	Transverse rupture strength, MPa	Fracture toughness, MPa · $M^{1/2}$
Si_3N_4 + (TiC + ZrN + Al_2O_3)	93.5	70	6

2. Experimental Procedures

The ceramic cutting tool used in this research was Si_3N_4 with dimensions of 13 by 13 by 8 mm, a rake angle of –6 to –7°, and a corner radius of 0.8 mm. Table 1 shows its chemical composition and mechanical properties. The relative densities are all >0.99. The microstructure (Fig. 1) consists mainly of a Si- and Al-rich core and is surrounded by the binder phases. The small grain size is <0.5 μm and the large ones are about 1 to 2 μm. The materials to be machined were 1045 plain carbon and 302 stainless steels. Their composition and mechanical properties are given in Table 2.

Cutting tests were carried out without coolant on a C620 lathe, and the cutting parameters were selected as follows: cutting speed 50 to 260 m/min, cutting depth 0.25 mm, feed rate 0.1 to 0.5 mm/revolution, and cutting distance 300 m.

The flank wear VB was measured using a tool maker's microscope. According to the measurement results, of more than 30 points at different cutting speeds and feed rates, the wear maps with different regions were obtained on the two-dimensional diagram. The wear morphologies and mechanisms in different regions were investigated by SEM with EDX analysis.

The temperature distribution on the flank face of a Si_3N_4 tool when cutting 1045 and 302 steels at the conditions of different cutting speeds and 0.1 mm/revolution feed rate was measured by the thermal video system TVS-2200. The details of this measurement and its data processing will be published in a subsequent paper (Ref 12).

3. Experimental Results and Discussions

3.1 *Wear Map of Si_3N_4 Tool for Cutting 1045 Steel and Wear Mechanisms*

Figure 2 shows the flank wear VB values at various cutting speeds and feed rate conditions. According to the ranges of

Table 2 Chemical composition and mechanical properties of the workpieces

Steel	C	Mn	Si	Cr	Ni	P	S	σ_b, N/mm²	δ, %	Hardness	λ, cal/cm · s °C
1045	0.45	0.65	0.27	≤0.25	≤0.25	≤0.04	≤0.04	610	16	241	0.120
1Cr18Ni9Ti	≤0.12	≤2.00	≤0.80	18.0	9.5	≤0.035	≤0.03	550	40	291	0.039

flank wear, four regions can be divided in the wear map. Region A shows the least wear (VB = 0.03 to 0.05 mm), with the cutting speed range of 95 to 128 m/min and the feed rate range of 0.2 to 0.3 mm/revolution. Region B shows a higher VB value of 0.06 to 0.07 mm. Considering comprehensively the tool life and productivity, region B can be regarded as an optimum machining condition. For region C, the VB values were up to 0.10 to 0.20 mm; whereas in region D, it increased significantly to >0.30 mm, where fracture occurred.

Figure 3(a-d) shows typical SEM morphologies of wear surface on the flank face at different regions. In regions A and B, the wear mechanisms were abrasive wear with the wear track corresponding to the friction direction. The severity of region B was larger than that of region A. In region C(I) (with lower speed and higher feed), the broken edge area was obvious; however, no adhesion was found at the area, as shown in its morphology, indicating that the broken edge was caused due to mechanical stress. In region C(II) (higher speed and higher feed), the adhesive metal fragment was displayed. When the conditions entered region D, the adhesion became more severe,

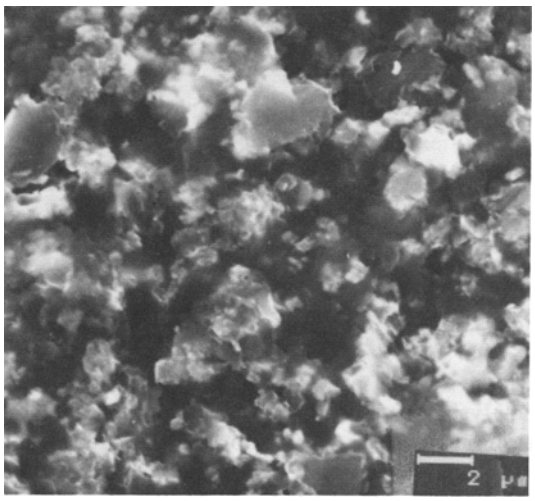

Fig. 1 The microstructure of a Si_3N_4 ceramic tool

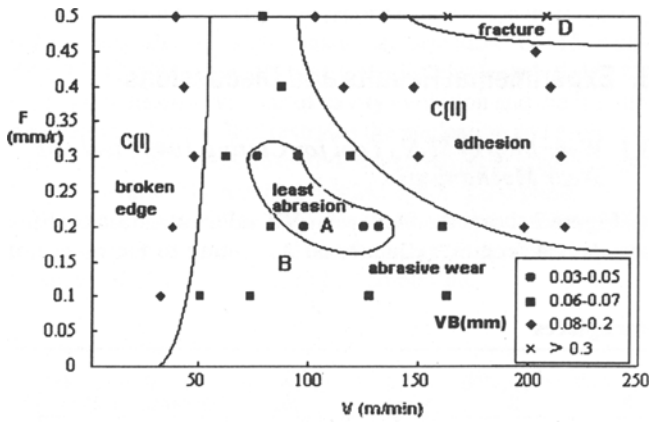

Fig. 2 Wear map of a Si_3N_4 ceramic tool when cutting 1045 steel

and it could usually pull some Si_3N_4 material by delamination as the adhesive metal was detached.

The wear mechanisms are closely related to the cutting temperature and cutting force near the tool edge. Figure 4 shows the temperature distribution on the flank face of the Si_3N_4 tool. Figure 5 shows the curves of temperature varied with the cutting speed. It can be found in region C(I) when the cutting speed was less than 50 m/min, the temperature was lower (<600 °C), and basically no adhesion occurred. However, at lower cutting speeds, the deformation coefficient ξ ($\xi = h_{ch}/h_D$, where h_{ch} is the thickness of the chip and h_D is the cutting depth) would be larger (Ref 13), and when the feed rate was higher, the cutting resistance also became larger. Therefore, this region was of low temperature and high force (LT&HF), and the tool edge could be easily broken due to mechanical stress. When the cutting speeds and feed rates reached the C(II) region, the VB values were almost the same as in region C(I); however, the wear mechanisms were different. In the C(II) region, the temperature was about 1000 to 1200 °C, and the cutting force was also larger at high feed rate, therefore it belongs to a region of high force and high temperature (HF&HT). These conditions would certainly promote adhesion at the tool-work interface. Analyzing the B region by the same method, we found that it covered quite a broad range of cutting speeds and feed rate, but the high cutting speed and high feed rate didn't exist at the same time, so adhesion was not present and abrasive wear was the main wear mechanism. In region A, the temperature was approximately 1000 °C, which could be considered as the optimum temperature condition where no adhesion occurred and the abrasive wear was also the least. In the D region, both the cutting force and temperature were maximum on the map, which would certainly cause severe adhesion, and when the adhesive metal detached from the flank face during the continuous turning, the tool material could be pulled out so that the fracture occurred.

3.2 *Wear Map of Si_3N_4 Tool for Cutting 302 Stainless Steel and Wear Mechanisms*

Figure 4 shows the wear map of the Si_3N_4 tool for cutting a 302 stainless steel at various cutting speeds and feed rates. Differing from the map for cutting 1045 steel, only three regions were found on this map. Region A showed the least flank wear range of 0.06 to 0.10 mm in the cutting speed range of 106.7 to 163.3 m/min and a feed rate range of 0.1 to 0.2 mm/revolution. The flank wear became more severe (>0.30 mm) when the feed rates were higher than 0.3 mm/revolution for all cutting speeds. Region B showed the medium flank wear at 0.11 to 0.25 mm. From these data, it can be determined that the flank wear of a Si_3N_4 tool for cutting stainless steel is obviously higher than that for cutting plain carbon steel.

Figure 7 displays the typical SEM morphologies of the wear surface on the flank face for different regions. The severe flank wear in region C is shown in Fig. 7c, and the microfracture can also be seen in Fig 7d. From the results of SEM and EDX analysis on the chip, as shown in Fig. 8, we can consider that the severe adhesion happened first, and then during the continuous turning the adhesive material was delaminated, which induced the peeling-off of the ceramic material. In region B, adhesion was severe and the whole flank face was nearly covered by the

adhesive workpiece material. There existed a small region A, which was suitable for cutting with the least adhesion and the abrasive wear was mild as well. The wear mechanisms can be explained also by the cutting temperature. Figure 9 shows the temperature distribution curves as measured by the thermal video system. The cutting temperature varied with cutting speed is shown in Fig. 5. Comparing it with Fig. 4, it is apparent that the cutting temperature for cutting stainless steel was approximately 20% higher than for cutting plain carbon steel; it can reach approximately 1400 °C at high cutting speed. Reasons for this phenomenon are due to the high toughness and ductility of stainless steel on one hand, which is about 1½

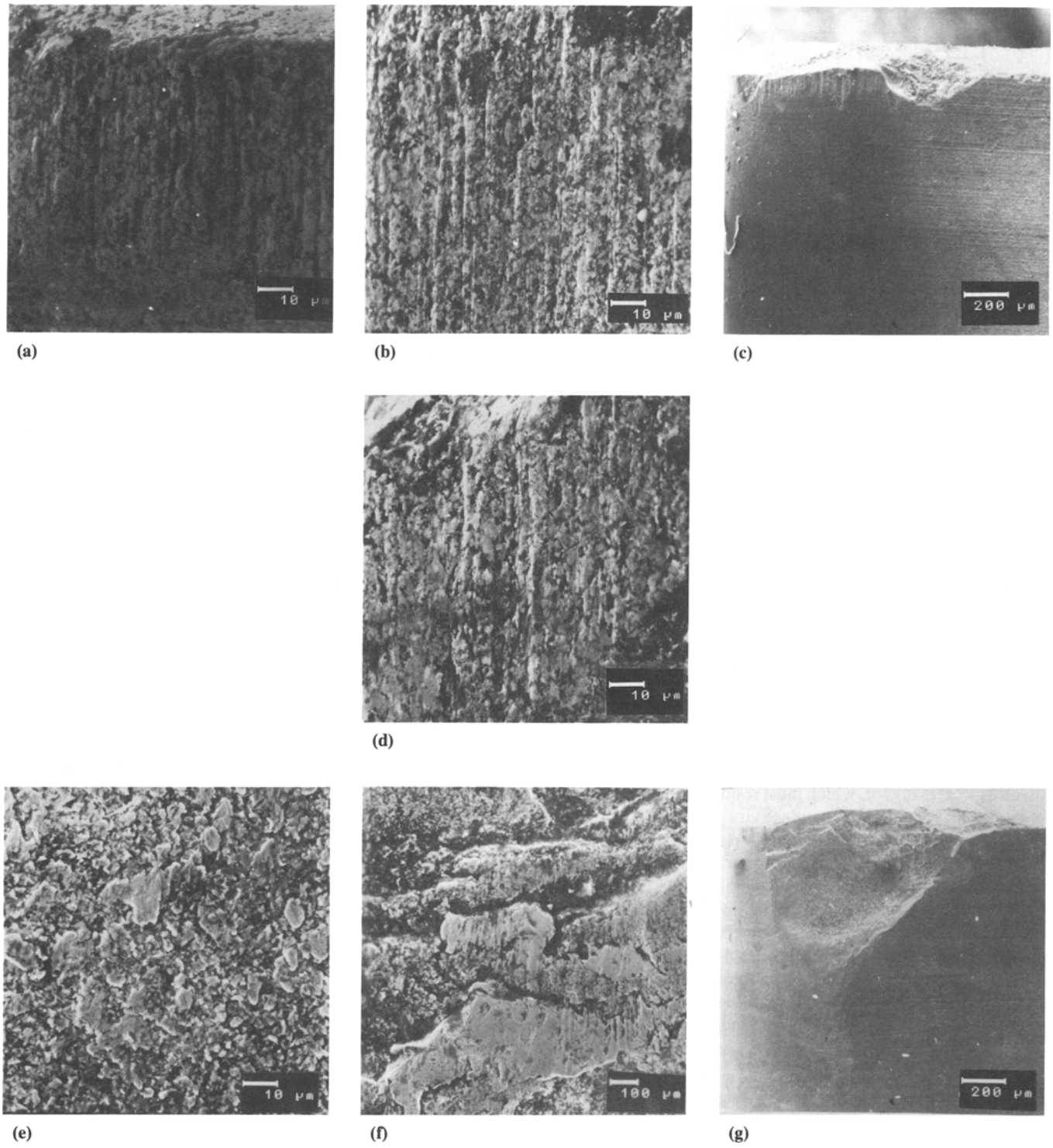

Fig. 3 Typical SEM morphologies of the wear surface of a Si_3N_4 ceramic tool when cutting 1045 steel. (a) Region A. (b) Region B. (c) Region C(I). (d) Region C(I). (e) Region C(II). (f) Region D. (g) Region D

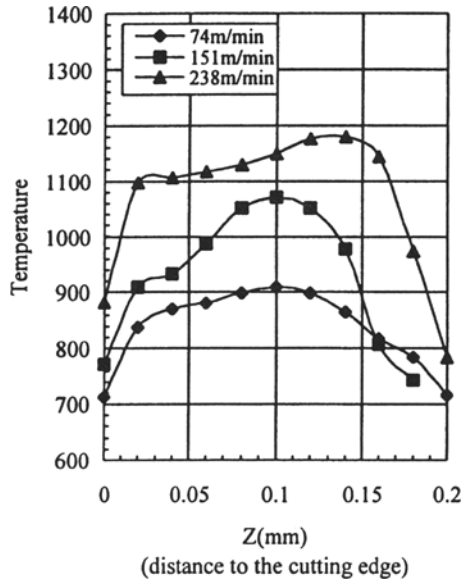

Fig. 4 The temperature distribution on the flank face of a Si_3N_4 ceramic tool when cutting 1045 steel

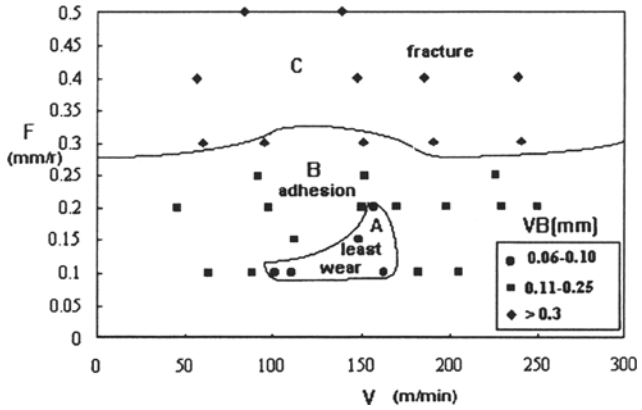

Fig. 6 Wear map of a Si_3N_4 ceramic tool when cutting 302 stainless steel

times that of 1045 steel (Ref 14), so the cutting resistance of stainless steel is higher, which must result in the higher cutting heat, and its poor thermal conductivity (K = 0.039 cal/cm.s), which is only one-third that of 1045 steel (Ref 15), on the other. Therefore the main wear mechanism for cutting stainless steel was adhesion promoted by high temperature.

The contact length between the chip and rake face, when cutting the stainless steel, was shorter. It was approximately 65 to 70% of the length when cutting 1045 steel (Ref 15). Thus, the higher cutting force and temperature can be concentrated on the cutting edge, which will easily make the ceramic tool subject to the high thermal shock and induce microfracture.

4. Conclusions

- The wear maps of a Si_3N_4 ceramic tool for cutting 1045 plain carbon and 302 stainless steels were obtained according to the cutting parameters in region A, which can be suggested for less wear and longer tool life.
- The flank wear of a Si_3N_4 ceramic tool when cutting 302 stainless steel was always higher than that for cutting 1045 plain carbon steel due to the higher cutting temperature of the former.
- The main wear mechanisms of a Si_3N_4 ceramic tool were microfracture and abrasive wear in the condition of lower cutting speeds, and adhesion-induced fracture and delamination at higher cutting speeds. An optimum region, where

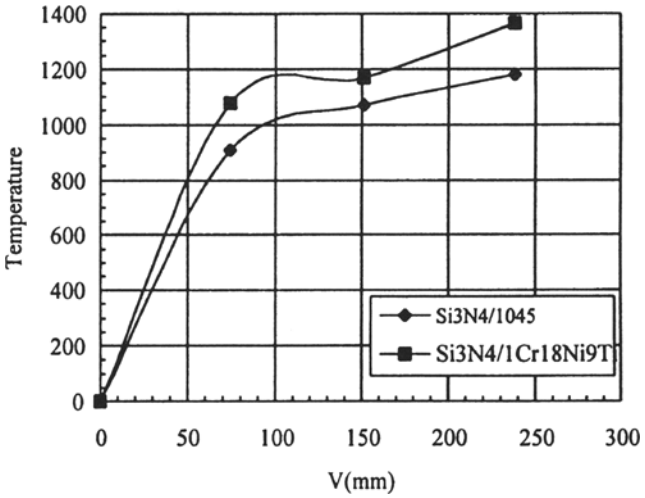

Fig. 5 The curves of temperature varied with cutting speed

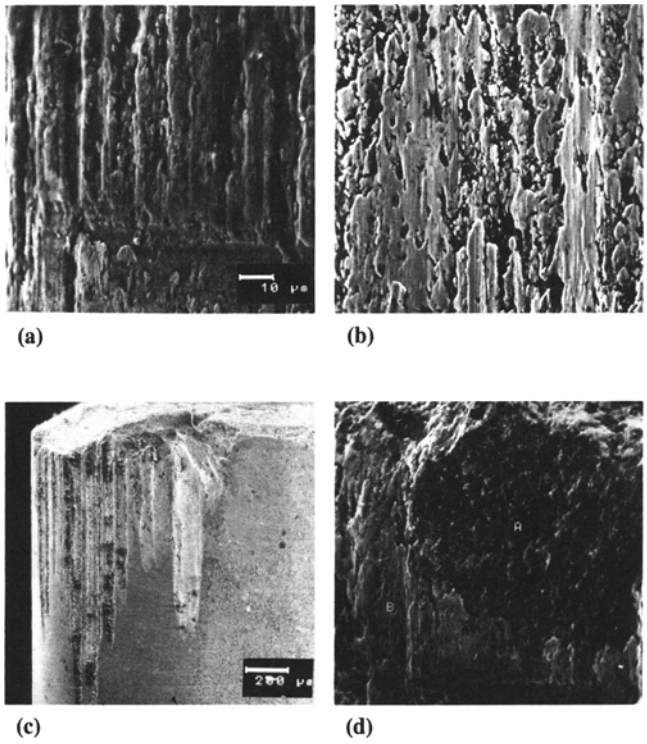

Fig. 7 Typical SEM morphologies of the wear surface of a Si_3N_4 ceramic tool when cutting 302 stainless steel. (a) Region A. (b) Region B. (c) Region C. (d) Region D

(a)

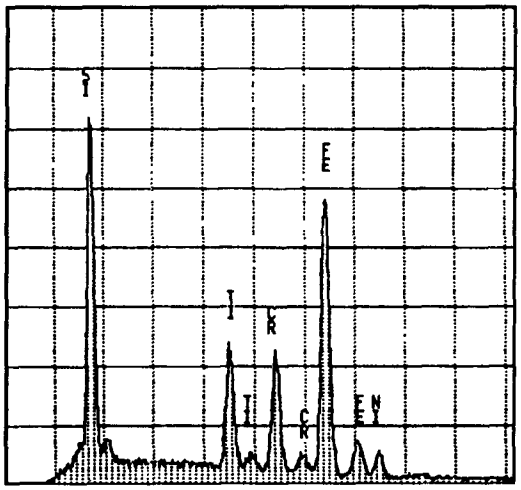

(b)

Fig. 8 SEM morphology of chip (a) and its EDX analysis (b)

both fracture and adhesion were not obviously developed, is always present at medium cutting speed.

- The cutting temperature was measured by a thermal video system. The temperature distribution on the Si_3N_4 tool surface when cutting 302 steel was approximately 20% (on average) higher than when cutting 1045 steel. The high cutting temperature could easily promote adhesion and adhesion-induced failures of the ceramic tool.

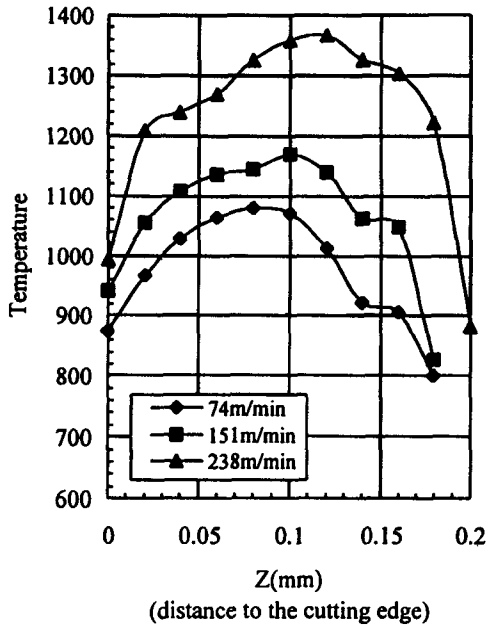

Fig. 9 Temperature distribution on the flank face of a Si_3N_4 ceramic tool when cutting 302 stainless steel

Acknowledgment

This research was supported financially by the National Natural Science Foundation and Lanzhou Institute of Chemical Physics, Academy of Sciences.

References

1. M. Masuda, Cutting Performance and Wear Mechanism of Alumina-Base Ceramic Tools When Machining Austempered Ductile Iron, *Wear,* Vol 174, 1994, p 147-153
2. S.L. Casto, Wear Performance of Ceramic Cutting Tool Materials When Cutting Steel, *J. Mater. Process. Technol.,* Vol 28, 1991, p 25-36
3. N. Richards, Use of Ceramic Tools for Machining Nickel-Base Alloys, *Int. J. Mach. Tools Manuf.,* Vol 29 (No. 4), 1989, p 575-588
4. D.H. Jack, Ceramic Cutting Tool Materials, *Mater. Des.,* Vol 5, 1986, p 25-33
5. H. Thoors and H. Chandraselaran, Study of Some Active Wear Mechanisms in a Titanium-Base Cermet When Machining Steels, *Wear,* Vol 162-164, 1993, p 1-11
6. S.F. Wangne and S.T. Bulian, The Role of Thermal Shock on Life of Selected Ceramic Cutting Tool Materials, *J. Am. Ceram.,* Vol 72 (No. 5), 1989, p 754-760
7. J. Aucote and S.R. Foster, Performance of Sialon Cutting When Machining Nickel-Base Aerospace Alloys, *J. Mater. Sci.,* Vol 2, 1986, p 700-708
8. S.L. Casto and L. Valco, Wear Mechanism of Ceramic Tools, *Wear,* Vol 160, 1993, p 227-235
9. S.T. Buljan, Wear and Design of Ceramic Cutting Tool Materials, *Wear,* Vol 133, 1989, p 309-321
10. S.F. Wayne, Wear of Ceramic Cutting Tools in Ni-Base Superalloy Machining, *Tribol. Trans.,* Vol 33 (No. 4), 1990, p 618-626
11. T.N. Blackman, Developments in Machining of Cast Iron, *Foundryman,* Vol 1, 1990, p 17-24
12. Y.-R. Liu and J.-J. Liu, The Temperature Distribution Near Cutting Edge of Ceramic Cutting Tools Measured by the Thermal Video System, *J. Prog. Nat. Sci.,* 1997, in press
13. R.B. Ross, *Metallic Materials Specification Handbook,* E. & F.N. Son. Ltd., 1980
14. *ASM Metals Reference Book,* American Society for Metals, 1984
15. Q.-F. Li, *Machining Technology of Difficult-to-Machine Materials,* Beijing Press of Science and Technology, 1992